

Please cite the Published Version

Kowalczyk, PS (2017) A novel route to a Hopf bifurcation scenario in switched systems with dead-zone. *Physica D: Nonlinear Phenomena*, 348. pp. 60-66. ISSN 0167-2789

DOI: <https://doi.org/10.1016/j.physd.2017.02.007>

Publisher: Elsevier

Version: Accepted Version

Downloaded from: <https://e-space.mmu.ac.uk/617998/>

Usage rights:  [Creative Commons: Attribution-Noncommercial-No Derivative Works 4.0](https://creativecommons.org/licenses/by-nc-nd/4.0/)

Additional Information: This is an Author Accepted Manuscript provided by Elsevier of a paper accepted for publication in *Physica D: Nonlinear Phenomena*.

Enquiries:

If you have questions about this document, contact openresearch@mmu.ac.uk. Please include the URL of the record in e-space. If you believe that your, or a third party's rights have been compromised through this document please see our Take Down policy (available from <https://www.mmu.ac.uk/library/using-the-library/policies-and-guidelines>)

A novel route to a Hopf bifurcation scenario in switched systems with dead-zone

P. Kowalczyk *

November 11, 2016

Abstract

Planar switched systems with dead-zone are analyzed. In particular, we consider the effects of a perturbation which is applied to a linear control law and, due to the perturbation, the control changes from purely positional to position-velocity control. This type of a perturbation leads to a novel Hopf-like discontinuity induced bifurcation. We show that this bifurcation leads to the creation of a small scale limit cycle attractor, which scales as the square root of the bifurcation parameter. We then investigate numerically a planar switched system with a positional feedback law, dead-zone and time delay in the switching function. Using the same parameter values as for the switched system without time delay in the switching function, we show a Hopf-like bifurcation scenario which exhibits a qualitative and a quantitative agreement with the scenario analyzed for the non-delayed system.

Keywords: Non-smooth bifurcations, Hopf bifurcations, switched control systems

1 Introduction

Dynamical systems which are characterized by switchings between a number of distinct differentiable vector fields, with the switching law that depends on the value of some state variable, are common in engineering applications (e.g. control or mechanical engineering [2, 5, 26, 8, 22]). Such systems, depending on the context, are termed as hybrid dynamical systems, non-smooth systems, or switched systems. In recent years, much of research effort has been spent on classifying bifurcations, termed as discontinuity induced bifurcations - DIBs for short, specifically pertaining to systems with switched vector fields, see for some examples [16, 15, 6, 13, 4, 18]. However, unlike in the case of n -dimensional differentiable vector fields a complete theory of bifurcation scenarios (e.g. local bifurcations of co-dimension one) in non-smooth systems has, as yet, not been possible. Switched (or hybrid systems) can be seen as a concatenation of differentiable vector fields in a way which is dependent on the class of switched systems under investigation. Hence the structure of phase space in non-smooth systems allows a plethora of different configurations even in the case of low dimensional systems. For this reason, bifurcations in non-smooth systems are treated by considering non-smooth (hybrid systems) with a switching law that has a certain specific structure and thus the conditions that define a switching law provide restrictions as to what types of bifurcations could occur in a given class of switched (hybrid) systems.

*School of Computing, Mathematics and Digital Technology, John Dalton Building, Manchester Metropolitan University, Chester Street, Manchester, M1 5GD, U.K., Email: p.kowalczyk@mmu.ac.uk

Recently, it has been suggested that the presence of switched or intermittent control induces sway dynamics during quiet standing of humans [20, 1, 11, 12]. One way of verifying this hypothesis is to investigate the dynamics of switched models in the context of human balance as presented in [20, 1, 14, 12, 19]. In particular, the authors in [20, 1, 14, 12, 19] consider different types of switched control laws to account for sway patterns observed experimentally, and the dynamics of these models is investigated. In [1] phase space is divided into different adjacent regions where the control action is either switched on or off. The authors argue that the convergence to upright equilibrium during quiet standing is linked with the neuromuscular system directing the body to follow the stable manifold of the saddle type “upright” equilibrium. In [14] a multistability and homoclinic bifurcation scenario in a switched model with dead-zone and the delay in state variables is shown. The models with dead-zone and time delay in the switching function and state variables are further analyzed in [25] where homoclinic bifurcations, complex bursting dynamics and so-called boundary bifurcations are investigated. Another context of human neuromuscular control where switched models could be applied is in modeling variations of threshold detection due to diabetes or aging. Motivated by the above mentioned applications, in the current paper, we consider planar switched systems with dead-zone. In particular, within the dead-zone the equations of motions describe an inverted pendulum model and outside of the dead-zone a position or position-velocity control is applied to the inverted pendulum model system. The contribution of the current work is the analysis of a novel type of a Hopf-like bifurcation scenario as yet not analyzed in the literature triggered by a perturbation from position to position-velocity control. We also link this bifurcation with a Hopf-like bifurcation, first time reported in the current work, in the system with dead-zone, purely positional feedback law and delay in the switching decision function.

The rest of the paper is outlined as follows. In Sec. 2 switched systems with dead-zone that we analyze in the paper are introduced. We then, in Sec. 3, analyze a Hopf-bifurcation ensuing in the system due to a perturbation of the control vector using asymptotic method. The existence and stability analysis of a small scale limit cycle born in the bifurcation is shown in Sec. 4. We then proceed in Sec. 5 to verify our analytical results by means of numerical investigations of the system around the bifurcation point. In the following Sec. 6, using a system with time delay in the switching function we numerically investigate a Hopf-like bifurcation which shows qualitative and quantitative agreement with the Hopf-like scenario of the non-delayed system. We then provide a brief theoretical explanation for the observed agreement. Finally, Sec. 7 concludes the paper.

2 Systems of interest

Consider a class of systems given by

$$\dot{x} = A_I x \quad \text{for} \quad |Cx| \leq \phi, \quad (1)$$

$$\dot{x} = A_O x \quad \text{for} \quad |Cx| > \phi, \quad (2)$$

where $A_I \in \mathbb{R}^2 \times \mathbb{R}^2$ is a non-singular matrix with the eigenvalues corresponding to a saddle-node equilibrium point, and $A_O \in \mathbb{R}^2 \times \mathbb{R}^2$ is a non-singular matrix with the eigenvalues corresponding to a stable equilibrium point of the focus type. The product of the state vector $x \in \mathbb{R}^2$ and the constant control row vector $C \in \mathbb{R}^2$ determines the switching between the two linear vector fields for some fixed and positive value of ϕ . In what follows, we consider a novel Hopf bifurcation scenario in the above class of systems under the variation of the control vector from $C = C_0$ to $C = C_0^\epsilon$.

2.1 Planar switched systems with dead-zone

Consider switched systems where the bifurcation parameter, say β , is increased from 0 and implies a change of the control vector C_0 from $C_0 = [-1 \ 0]$ to $C_0^\epsilon = [-1 \ \beta]$, where $\beta = \mathcal{O}(\epsilon)$. This variation is a change from purely positional feedback control law to position-velocity feedback law. Matrices A_I , A_O , the state vector \mathbf{x} and the width of the dead-zone are given by

$$A_I = \begin{pmatrix} 0 & 1 \\ A & 0 \end{pmatrix}, \quad A_O = \begin{pmatrix} 0 & 1 \\ A - K_p & -K_d \end{pmatrix}, \quad \mathbf{x} = \begin{pmatrix} \theta \\ \dot{\theta} \end{pmatrix}, \quad |C_0 \mathbf{x}| \leq \theta^*, \text{ or } |C_0^\epsilon \mathbf{x}| \leq \theta^*, \quad (3)$$

where $K_p > A > 0$, $K_p - A > K_d^2/4$, $K_d > 0$ and $\theta^* > 0$. In this set up the eigenvalues of A_I correspond to the system's equilibrium point of a saddle type and the eigenvalues of A_O correspond to a stable focus, as assumed earlier. Matrix A_I is expressed in so-called controllable canonical form [3, 7] and this structure can be assumed without loss of generality

2.2 Phase space topology

We now define switching manifolds Σ_\pm and Σ_\pm^ϵ as

$$\Sigma_\pm = \{(\theta, \dot{\theta}) \in \mathbb{R}^2 : \pm\theta^* - \theta = 0\}, \quad (4)$$

$$\Sigma_\pm^\epsilon = \{(\theta, \dot{\theta}) \in \mathbb{R}^2 : \beta\dot{\theta} \pm \theta^* - \theta = 0\} \quad (5)$$

and regions

$$G_{IN} = \{(\theta, \dot{\theta}) \in \mathbb{R}^2 : |\theta| < \theta^*\}, \quad (6)$$

$$G_{OUT} = \{(\theta, \dot{\theta}) \in \mathbb{R}^2 : |\theta| > \theta^*\}, \quad (7)$$

$$G_{IN}^\epsilon = \{(\theta, \dot{\theta}) \in \mathbb{R}^2 : |\beta\dot{\theta} - \theta| < \theta^*\}, \quad (8)$$

$$G_{OUT}^\epsilon = \{(\theta, \dot{\theta}) \in \mathbb{R}^2 : |\beta\dot{\theta} - \theta| > \theta^*\}. \quad (9)$$

The flow within region G_{IN} or G_{IN}^ϵ , say ψ_{IN} , is given by the solution of the differential equation

$$\ddot{\theta} - A\theta = 0, \quad (10)$$

and the flow within region G_{OUT} or G_{OUT}^ϵ , say ψ_{OUT} , is given by the solution of

$$\ddot{\theta} + K_d\dot{\theta} + (K_p - A)\theta = 0. \quad (11)$$

Finally, define

$$H(\theta, \dot{\theta}) = \beta\dot{\theta} + \theta^* - \theta. \quad (12)$$

Clearly, the zero level set of H defines the switching manifold Σ_+^ϵ .

3 Local stability calculations

It has been shown in [14] that the system dynamics with the switching law given by $C_0 \mathbf{x} = \pm\theta^*$ is governed by the existence of a pair of stable pseudo-equilibria $EQ_\pm = (\pm\theta^*, 0)$. We define a pseudo-equilibrium point in the switched system (1) and (2) as a point $EQ \in \Sigma_\pm$ such that for some t_0 $(\pm\theta^*(t_0), 0) \in \Sigma_\pm$ and $\forall t \geq t_0$ $(\pm\theta(t), 0) = (\pm\theta^*(t_0), 0)$. We note that considering only forward time suffices for our purposes. The pseudo-equilibria $(\pm\theta^*(t_0), 0) \in \Sigma_\pm$ have been shown to be the only two global attractors of the system. If we now “switch on” the control vector C_0^ϵ the two pseudo-equilibria lose their stability and there is born a pair of stable limit cycles with the amplitude which grows in the $\mathcal{O}(\sqrt{\beta})$. Hence a Hopf-like bifurcation takes place in the system. Due to the system's symmetry the Hopf-bifurcation occurs simultaneously around both pseudo-equilibria. It is sufficient to consider the Hopf bifurcation around one of the two pseudo-equilibria. In what follows we will concentrate on EQ_+ .

3.1 Calculating flow time τ

Consider initial point, say $P_0 = (\theta(0), \dot{\theta}(0)) \in \Sigma_+^\epsilon$, such that $\dot{\theta}(0) = \dot{\theta}_0 = \mathcal{O}(\epsilon)$. It then follows that $\theta^* - \theta_0 = -\beta\dot{\theta}_0 = \mathcal{O}(\epsilon^2)$.

If $\theta^* - \theta_0 > 0$ and $\beta > 0$ then $\dot{\theta}_0 < 0$ and the flow within the dead-zone, in the neighborhood of the pseudo-equilibrium, is governed by the solution of

$$\ddot{\theta} - A\theta = 0,$$

which, clearly, is given by

$$\theta(\tau) = C_1 \exp(-\sqrt{A}\tau) + C_2 \exp(\sqrt{A}\tau) \quad (13)$$

$$\dot{\theta}(\tau) = -\sqrt{A}C_1 \exp(-\sqrt{A}\tau) + \sqrt{A}C_2 \exp(\sqrt{A}\tau). \quad (14)$$

Using the initial conditions we find

$$\theta(\tau) = \frac{\sqrt{A}\theta_0 - \dot{\theta}_0}{2\sqrt{A}} \exp(-\sqrt{A}\tau) + \frac{\sqrt{A}\theta_0 + \dot{\theta}_0}{2\sqrt{A}} \exp(\sqrt{A}\tau) \quad (15)$$

$$\dot{\theta}(\tau) = -\frac{\sqrt{A}\theta_0 - \dot{\theta}_0}{2} \exp(-\sqrt{A}\tau) + \frac{\sqrt{A}\theta_0 + \dot{\theta}_0}{2} \exp(\sqrt{A}\tau). \quad (16)$$

We assume that the time, say τ , required for the flow to reach Σ_+^ϵ is $\tau = \mathcal{O}(\epsilon)$. We then get

$$\theta(\tau) = \theta_0 - \frac{\theta^* - \theta_0}{\beta} \tau + \frac{1}{2} A \theta_0 \tau^2 + \mathcal{O}(\epsilon^3), \quad (17)$$

$$\dot{\theta}(\tau) = A \theta_0 \tau - \frac{\theta^* - \theta_0}{\beta} + \mathcal{O}(\epsilon^2). \quad (18)$$

Solving $H = 0$ for τ , to leading order in τ , gives

$$\tau = 2\beta + \frac{2(\theta^* - \theta_0)}{A\theta_0\beta} + \mathcal{O}(\epsilon^2). \quad (19)$$

Thus the point of intersection with Σ_+^ϵ , say $P_1 \in \Sigma_+^\epsilon$, is given by

$$\theta_1 = \theta_0 + 2(\theta^* - \theta_0) + 2A\theta_0\beta^2 > \theta^*, \quad (20)$$

$$\dot{\theta}_1 = 2A\theta_0\beta + \frac{\theta^* - \theta_0}{\beta} > 0. \quad (21)$$

3.2 Calculating flow time δ

We now need to find the flow time, say δ , back to the switching line Σ_+^ϵ following the ψ_{OUT} flow, which is given by the solution of the differential equation (11)

$$\ddot{\theta} + K_d \dot{\theta} + (K_p - A)\theta = 0.$$

Assume $\delta = \mathcal{O}(\epsilon)$ and let $a = K_d/2$ and $b = \sqrt{(K_p - A) - (K_d/2)^2}$.

We find the flow solutions

$$\theta(\delta) = \theta_1 \exp(-a\delta) \cos(b\delta) + \frac{\dot{\theta}_1 + a\theta_1}{b} \exp(-a\delta) \sin(b\delta) \quad (22)$$

$$\dot{\theta}(\delta) = \dot{\theta}_1 \exp(-a\delta) \cos(b\delta) - \frac{a\dot{\theta}_1 + a^2\theta_1 + b^2\theta_1}{b} \exp(-a\delta) \sin(b\delta). \quad (23)$$

Expanding to $\mathcal{O}(\epsilon^3)$ equation (22) for the angular position, and equation (23) for the angular velocity, we get

$$\theta(\delta) = \theta_1 - \frac{1}{2}(a^2 + b^2)\theta_1\delta^2 + \dot{\theta}_1\delta + \mathcal{O}(\epsilon^3) \quad (24)$$

$$\dot{\theta}(\delta) = -(a^2 + b^2)\theta_1\delta + \dot{\theta}_1 + \mathcal{O}(\epsilon^2). \quad (25)$$

Inserting (20) and (21), for the initial position and velocity components, into (24) and (25) gives

$$\theta(\delta) = \theta_0 + 2(\theta^* - \theta_0) + 2A\theta_0\beta^2 - \frac{1}{2}(a^2 + b^2)\theta_0\delta^2 + \quad (26)$$

$$2A\theta_0\beta\delta + \frac{\theta^* - \theta_0}{\beta}\delta + \mathcal{O}(\epsilon^3)$$

$$\dot{\theta}(\delta) = -(a^2 + b^2)\theta_0\delta + 2A\theta_0\beta + \frac{\theta^* - \theta_0}{\beta} + \mathcal{O}(\epsilon^2). \quad (27)$$

We may now use the above expressions and insert them in the equation for the switching line (12). We find the time δ

$$\delta = 2 \frac{(a^2 + b^2 + 2A)\theta_0\beta^2 + \theta^* - \theta_0}{\beta(a^2 + b^2)\theta_0} + \mathcal{O}(\epsilon^2), \quad (28)$$

which is well-defined since $a^2 + b^2 = K_p - A > 0$, $\beta = \mathcal{O}(\epsilon) > 0$ and $\theta_0 > 0 = \mathcal{O}(1)$. Inserting for the time δ equation (28) into equations (26) and (27) for position and velocity, we finally find

$$\theta(\delta) = \theta_0 - 2\theta_0\beta^2(a^2 + b^2 + A) + \mathcal{O}(\epsilon^3) < \theta_0 \quad (29)$$

$$\dot{\theta}(\delta) = -2\theta_0\beta(a^2 + b^2 + A) - \frac{\theta^* - \theta_0}{\beta} + \mathcal{O}(\epsilon^2) < -\frac{\theta^* - \theta_0}{\beta}, \quad (30)$$

which indicates expansion and hence loss of stability of the pseudo-equilibrium $PS = (\theta^*, 0)$ for small positive β .

4 Small scale stable oscillations

4.1 Existence of the limit cycles

To determine the existence and stability of small scale oscillations born in the bifurcation, we may use the Hamiltonian function (similarly as in [14])

$$L(\theta, \dot{\theta}) = \frac{1}{2}\dot{\theta}^2 - \frac{1}{2}A\theta^2. \quad (31)$$

Consider an initial point, say $P_1(\theta_1, \dot{\theta}_1) \in \Sigma_+^\epsilon$, such that $\dot{\theta}_1 = -\frac{\theta^* - \theta_1}{\beta} > 0$. We seek to find the final point, say P_2 , such that $\Delta L = L(P_2) - L(P_1) = 0$ and $P_2 \in \Sigma_+^\epsilon$. We call the flow time from P_1 to P_2 by δ . If a limit cycle is born in the bifurcation, the order of magnitude of $\dot{\theta}_1$, θ_1 and δ can be determined by considering the geometry of flows ψ_{IN} and ψ_{OUT} with respect to Σ_+^ϵ in a sufficiently small neighbourhood of the pseudo-equilibrium point EQ_+ . Flow ψ_{IN} exhibits a quadratic tangency with respect to Σ_+^ϵ in some sufficiently small neighbourhood of EQ_+ . It can be shown that the time required to reach Σ_+^ϵ from some point, within the dead zone sufficiently close to EQ_+ , where flow ψ_{IN} attains its minimum with respect to Σ_+^ϵ , say $(\theta_0, \dot{\theta}_0)$, is of $\mathcal{O}(\sqrt{-(\theta_0 - \theta^*)})$. Thus the time of flight from Σ_+^ϵ back to itself under ψ_{IN} must be of $\mathcal{O}(\sqrt{-(\theta_0 - \theta^*)})$. We note here that the segment generated by ψ_{IN} can be characterized

by the sum of a section which can be found by flowing forward in time from $(\theta_0, \dot{\theta}_0)$ until Σ_+^ϵ and a second section by flowing backward in time towards Σ_+^ϵ . Obviously, in either case, due to the quadratic tangency of flow ψ_{IN} , we have the same order of magnitude. It then follows that the periodic point $(\theta_1, \dot{\theta}_1)$ is $(\mathcal{O}(1), \mathcal{O}(\sqrt{\epsilon}))$ respectively, and flow time $\delta = \mathcal{O}(\sqrt{\epsilon})$. The same geometry with respect to Σ_+^ϵ holds for flow ψ_{OUT} and thus the scaling law is preserved (see the Appendix for further details). We note that the somehow “unnatural” $\mathcal{O}(\sqrt{\epsilon})$ scaling arises due to the quadratic tangencies of both flows with respect to Σ_+^ϵ , exactly in the same manner as in the case of grazing bifurcations, or grazing-sliding bifurcations (in particular see, for example, the Appendix B in [21] for similar derivations). The expansions for the flows are “standard” power series expansions. We should note here that the degeneracies of matrices A_I and A_O may lead to the loss of the geometry described above and the introduced orders may no longer hold, and the bifurcation may altogether change its character.

Along any given segment of trajectory generated by flow ψ_{IN} there is no change in the value of Hamiltonian L . We use flow ψ_{OUT} and in particular equations (24) and (25) to determine point P_2 . Thus

$$\begin{aligned} \Delta L = & \frac{1}{2}(-(a^2 + b^2)\theta_1\delta + \dot{\theta}_1)^2 - A\frac{1}{2}(\theta_1 - \frac{1}{2}(a^2 + b^2)\theta_1\delta^2 + \dots \\ & + \dot{\theta}_1\delta)^2 - (\frac{1}{2}\dot{\theta}_1^2 - \frac{1}{2}A\theta_1^2), \end{aligned} \quad (32)$$

where $(\theta_1, \dot{\theta}_1) \in \Sigma_+^\epsilon$. We can write ΔL up to and including terms of $\mathcal{O}(\epsilon)$. We have

$$\begin{aligned} \Delta L = & \frac{1}{2}((a^2 + b^2)^2\theta_1^2\delta^2 + \dot{\theta}_1^2 - 2(a^2 + b^2)\theta_1\dot{\theta}_1\delta) + \dots \\ & - A\frac{1}{2}(\theta_1^2 - \theta_1^2\delta^2(a^2 + b^2) + 2\theta_1\dot{\theta}_1\delta) - \frac{1}{2}\dot{\theta}_1^2 + \frac{1}{2}A\theta_1^2. \end{aligned} \quad (33)$$

Simplifying (33) we get

$$\Delta L = -[(a^2 + b^2) + A]\theta_1\dot{\theta}_1\delta + \frac{1}{2}(a^2 + b^2)\theta_1^2\delta^2[(a^2 + b^2) + A], \quad (34)$$

which after further simplifications leads to

$$\Delta L = (-\dot{\theta}_1 + \frac{1}{2}K_p(K_p - A)\theta_1\delta)K_p\theta_1\delta. \quad (35)$$

Using (34) we can solve $\Delta L = 0$ for δ , which to leading order in ϵ gives

$$\delta = \frac{2\dot{\theta}_1}{(K_p - A)\theta_1} + \mathcal{O}(\epsilon). \quad (36)$$

We also require $(\theta_1, \dot{\theta}_1) \in \Sigma_+^\epsilon$ and $(\theta_2, \dot{\theta}_2) \in \Sigma_+^\epsilon$. Using equation (25) for the velocity $\dot{\theta}$ and inserting it into equation for the switching line Σ_+^ϵ given by (12), we find

$$\beta\dot{\theta}_1 + \theta^* - \theta_1 + \frac{1}{2}(K_p - A)\theta_1\delta^2 - \dot{\theta}_1\delta + \mathcal{O}(\epsilon^{3/2}) = 0, \quad (37)$$

where $\mathcal{O}(\epsilon^{3/2})$ signifies the remaining terms of $\mathcal{O}(\epsilon^{3/2})$ and higher. Note that $\beta\dot{\theta}_1 + \theta^* - \theta_1 = 0$, but $\beta\dot{\theta}_1 = \mathcal{O}(\epsilon^{3/2})$ and $\theta^* - \theta_1 = \mathcal{O}(\epsilon^{3/2})$. Thus the point $(\theta_2, \dot{\theta}_2) \in \Sigma_+^\epsilon$.

4.2 Stability calculations

To determine the stability of the limit cycle, we compute

$$\frac{d\Delta L}{d\dot{\theta}_1} = \frac{\partial \Delta L}{\partial \dot{\theta}_1} + \frac{\partial \Delta L}{\partial \delta} \frac{d\delta}{d\dot{\theta}_1}.$$

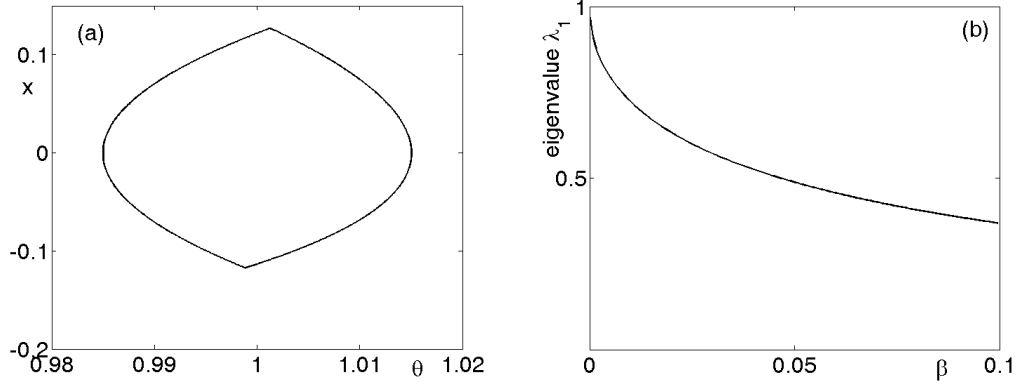


Figure 1: (a) A limit cycle attractor. (b) The variation of the non-trivial Floquet multiplier of the limit cycle attractor against the parameter β .

Using

$$H(\dot{\theta}_1, \delta) = 0$$

and applying the Implicit Function Theorem, we find

$$\frac{d\delta}{d\dot{\theta}_1} = -\frac{\partial H}{\partial \dot{\theta}_1} \left(\frac{\partial H}{\partial \delta} \right)^{-1}.$$

Using (36) for δ , we have

$$\frac{d\Delta L}{d\dot{\theta}_1} = -\frac{2K_p\dot{\theta}_1}{K_p - A} - K_p\theta_1\dot{\theta}_1\frac{d\delta}{d\dot{\theta}_1} + 2K_p\theta_1\dot{\theta}_1\frac{d\delta}{d\dot{\theta}_1}, \quad (38)$$

and so we find

$$\frac{d\delta}{d\dot{\theta}_1} = \frac{2}{(K_p - A)\theta_1}$$

to leading order.

Thus (38) simplifies to

$$\frac{d\Delta L}{d\dot{\theta}_1} = -\frac{K_p\dot{\theta}_1}{K_p - A} < 0 \quad (39)$$

to leading order, and hence the limit cycle born in the bifurcation is stable.

5 Numerical verification

In the following section, we numerically verify the analytical results described in the former section. In Fig. 1(a), we are depicting the limit cycle attractor born in the switched system for $\beta = 0.01$, $A = 0.5$, $K_p = 1$, $K_d = 1$ and $\theta^* = 1$. In Fig. 1(b), we depict variation of the non-trivial Floquet multiplier corresponding to the limit cycle attractor as a function of parameter β . The non-trivial Floquet multiplier lies within the unit circle of the complex plane, and hence we get further numerical verification that the limit cycle born in the bifurcation is a stable orbit.

An orbit diagram where we depict the variation of the maximum value of $\dot{\theta}$ on the limit cycle, say $|x_{\max}|$, versus β is then shown in Fig. 2(a).

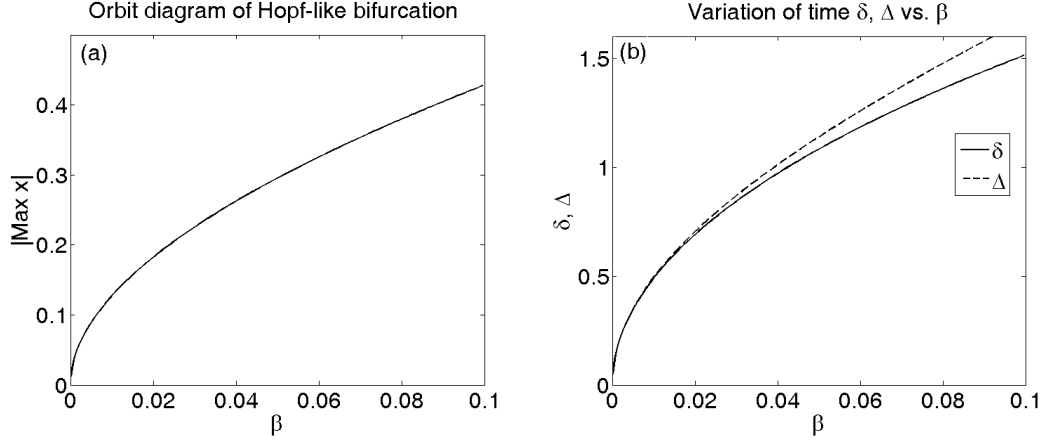


Figure 2: (a) Bifurcation diagram depicting $|x_{\max}|$ vs. β on the limit cycle born in the Hopf bifurcation. (b) Time variation of the duration of one segment, generated by flow ϕ_1 , making up the limit cycle born in the Hopf bifurcation using numerical (Δ) and asymptotic values (δ given by equation (36)).

In Fig. 2(a), we can clearly see the square root variation in the maximum value of the $\dot{\theta} = |x_{\max}|$ component as a function of the bifurcation parameter β . Then in Fig. 2(b), the time variation required to generate a segment of the limit cycle by the flow ψ_{OUT} as a function of parameter β is compared with numerical values. Asymptotic convergence is clearly visible.

6 Limit cycle attractor born due to delayed switching

6.1 System with delayed switching line and positional feedback

In the context of human neuro-muscular control, there are always present neurological time delays. For example, in the context of human balance control, there is a time delay present in the system due to neural processing and muscle activation. Therefore, we will compare numerically the Hopf-like bifurcation that we analyzed for the planar case with the Hopf-like scenario that we observed in switched system with dead-zone and time delay in the switching decision function. Namely consider a planar switched system of the form

$$\ddot{\theta} - A\theta = 0, \quad |\theta(t - \tau)| \leq \theta^*, \quad (40)$$

$$\ddot{\theta} - A\theta = -K_p\theta - K_d\dot{\theta}, \quad |\theta(t - \tau)| > \theta^*, \quad (41)$$

where $\theta^* > 0$, $K_p > A > 0$, $K_d > 0$, $K_p - A > K_d^2/4$ and $\tau = \mathcal{O}(\epsilon) > 0$. That is we consider the same parameter space as in Sec. 5. Similarly the flow ψ_{IN} is the solution of (40) and the flow ψ_{OUT} is the solution of (41).

System (40) and (41) can be seen as a model for human balance control during quiet standing where the neural transmission and muscle activation delays are included in the delay of the switching decision function [1, 14]. The dead-zone in the model can be seen as being related to the finite accuracy of sensing [1, 14]. Define

$$\Sigma_+^{\psi_{IN}} = \{(\theta, \dot{\theta}) \in \mathbb{R}^2 : \theta = \theta_1(\tau) \text{ and } \dot{\theta} = \dot{\theta}_1(\tau)\}, \quad (42)$$

where

$$\begin{aligned}\theta_1(\tau) &= \frac{\sqrt{A}\theta_0 - \dot{\theta}_0}{2\sqrt{A}} \exp(-\sqrt{A}\tau) + \frac{\sqrt{A}\theta_0 + \dot{\theta}_0}{2\sqrt{A}} \exp(\sqrt{A}\tau), \\ \dot{\theta}_1(\tau) &= -\frac{\sqrt{A}\theta_0 - \dot{\theta}_0}{2} \exp(-\sqrt{A}\tau) + \frac{\sqrt{A}\theta_0 + \dot{\theta}_0}{2} \exp(\sqrt{A}\tau),\end{aligned}$$

are the images of the position and velocity states on Σ_+ , namely for $\theta_0 = \theta^*$ and $\dot{\theta}_0 \in \mathbb{R}$, under the evolution of ψ_{IN} for the small fixed time $\tau = \mathcal{O}(\epsilon)$.

Similarly, define

$$\Sigma_+^{\psi_{OUT}} = \{(\theta, \dot{\theta}) \in \mathbb{R}^2 : \theta = \theta_2(\tau) \text{ and } \dot{\theta} = \dot{\theta}_2(\tau)\}, \quad (43)$$

where

$$\begin{aligned}\theta_2(\tau) &= \theta_0 \exp(-a\tau) \cos(b\tau) + \frac{\dot{\theta}_0 + a\theta_0}{b} \exp(-a\tau) \sin(b\tau), \\ \dot{\theta}_2(\tau) &= \dot{\theta}_0 \exp(-a\tau) \cos(b\tau) - \frac{a\dot{\theta}_0 + a^2\theta_0 + b^2\theta_0}{b} \exp(-a\tau) \sin(b\tau),\end{aligned}$$

and $a^2 = K_d^2/4$, $b^2 = (K_p - A) - K_d^2/4$, $\theta_0 = \theta^*$ and $\dot{\theta}_0 \in \mathbb{R}$. Thus $(\theta_2, \dot{\theta}_2)$ are the images of the position and velocity states, for any initial conditions on Σ_+ , under the evolution of ψ_{OUT} for the small fixed time $\tau = \mathcal{O}(\epsilon)$. Since Σ_+ is a line and the flows ψ_{IN} and ψ_{OUT} are linear then $\Sigma_+^{\psi_{IN}}$ and $\Sigma_+^{\psi_{OUT}}$ are lines in the phase space $(\theta, \dot{\theta})$ which, generically, will cross in some neighborhood of $(\theta^*, 0)$ for sufficiently small delay time τ .

6.2 Numerical observations

We will investigate numerically a bifurcation in the model under the switching of the delay time τ . For $\tau = 0$, we have a switched model with purely positional control and dead-zone, which has two stable pseudo-equilibria as the only attractors (see Sec. 2 and [14]). For $\tau > 0$, we have a dynamical system which is infinite dimensional due to the fact that, to be able to determine the forward evolution, it is necessary to keep track of a segment of trajectory for θ state in the interval $[t - \tau, t]$. However, if certain genericity conditions are satisfied in our delayed switched model, the system dynamics reduces to the evolution of finite number of state variables (see [23, 24]). In particular, let t_1 be the time of evolution from any point $(\theta, \dot{\theta}) \in \Sigma_+^{\psi_{IN}}$, in some neighborhood of $(\theta^*, 0)$, to Σ_+ , and t_2 be the time of evolution from any point $(\theta, \dot{\theta}) \in \Sigma_+^{\psi_{OUT}}$ to Σ_+ .

Then for τ sufficiently small we may assume that $\tau < t_1$ and $\tau < t_2$. This implies that, assuming a limit cycle exists in some neighborhood of the point $(\theta^*, 0)$, the dynamics of the delayed switched system can be described locally by a smooth one-dimensional map $\Sigma_+^{\psi_{IN}} \mapsto \Sigma_+^{\psi_{IN}}$. Other Poincaré section, transversal to the limit cycle, can be chosen. What is important, however, is the reduction of an infinite dimensional system to a finite dimensional one. In what follows, we show numerical evidence that this reduction preserves also quantitative features. In other words, we will provide numerical evidence that a switched system with position-velocity control may in certain circumstances behave exactly like a switched system with purely positional control and delayed switching.

In Fig. 3, we depict a limit cycle attractor born in the system for $\tau = 0.01$, $A = 0.5$, $K_p = 1$, $K_d = 1$ and $\theta^* = 1$ and compare it to the limit cycle attractor born in the switched position-velocity system with $\beta = 0.01$. It can be seen that the two limit cycles are virtually indistinguishable. In Fig.4(a) we compare bifurcation diagrams of both systems under variations of β and τ from 0, and in Fig. 4(b) we verify the variation of the non-trivial Floquet multiplier born in the Hopf-like bifurcation in either system. A simple argument may be given explaining

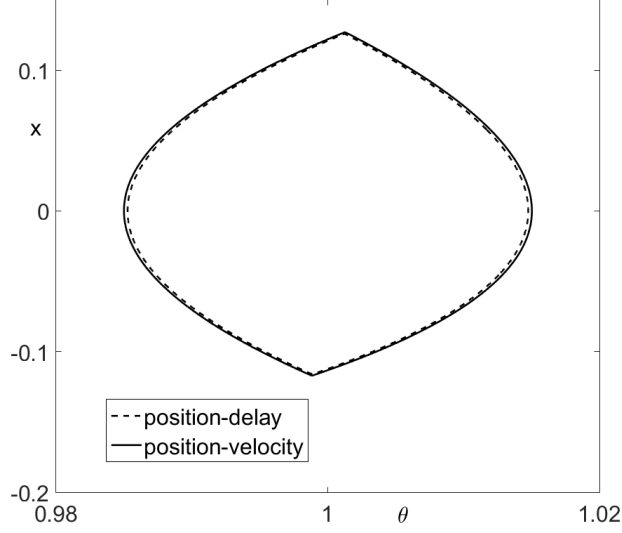


Figure 3: Limit cycle attractors born in Hopf-like bifurcation scenarios in switched (“position-velocity”) system (1) and (2) under the variation of the slope β (dashed line) and in system (40), (41) with the delayed switching line (“position-delay”) under the variation of the delay time τ (solid line).

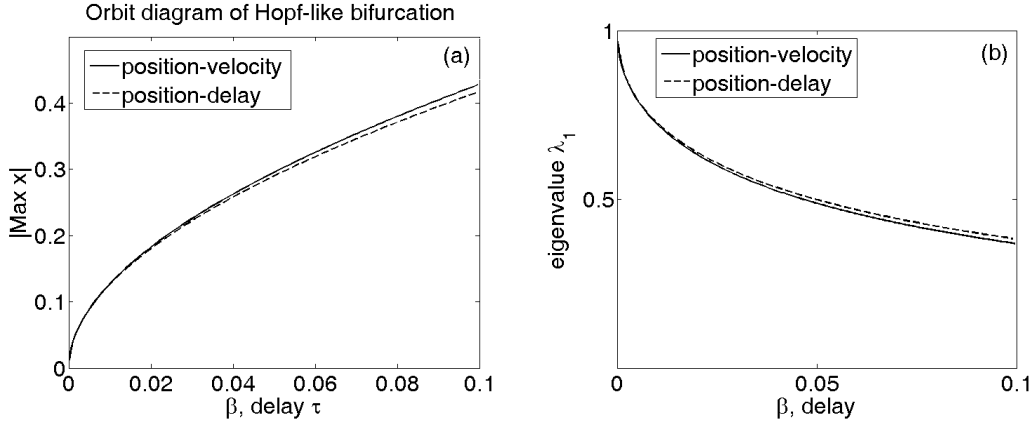


Figure 4: (a) A comparison between the variation of the non-trivial Floquet multiplier of the limit cycle attractor in the system with delayed switching line (dashed line) and no delay (solid line). (b) The variation of the non-trivial Floquet multiplier of the limit cycle attractor against the parameters β and time delay

the current situation. The delayed switching line is given by the expression $\theta(t - \tau) - \theta^* = 0$. Let us expand $\theta(t - \tau)$ in τ to leading order. That is, we obtain a switching line, which is given by $\theta(t) - \tau\dot{\theta}(t) - \theta^* = 0$. The algebraic expression for the switching line is now exactly the same as for the position-velocity switching line with τ taking the place of β . However, this holds for slowly oscillating orbits only, that is for orbits for which the flight time between switchings is greater than delay time δ . Now, in the delayed case the limit cycles, indeed, satisfy this condition since $\delta = \mathcal{O}(\sqrt{\epsilon})$ and $\tau = \mathcal{O}(\epsilon)$, and the delayed system reduces to the system with the position-velocity switching line for sufficiently small delay times τ .

7 Conclusions

In the paper, we analyze a novel type of a discontinuity induced bifurcation in the case when we apply a perturbation to the linear control feedback law. In particular, we show that switched linear systems with dead-zone and purely positional feedback under a small parameter perturbation, from position to position-velocity control, may lose a stable pseudo-equilibrium state (an equilibrium of the switched system which lies on the switching manifold) and produce a limit cycle in a Hopf-like scenario. Using asymptotic method we analyze this novel bifurcation and show the loss of stability of the pseudo-equilibrium and a birth of stable limit cycles with the amplitude, say $|x|$, growing as the square root of the bifurcation parameter ($|x| = \mathcal{O}(\sqrt{\beta})$, where β refers to the bifurcation parameter).

We then consider switched systems with dead-zone and purely positional feedback law, but with the switching decision function that contains time delay. We investigate this system numerically for small values of delay time $\tau = \mathcal{O}(\epsilon)$. We find that the system, considering the same parameter values as in the non-delayed case, exhibits a Hopf-like bifurcation scenario under the variation of τ , which not only qualitatively but also quantitatively matches the Hopf bifurcation in the switched system with no time delay. In control literature, it has been suggested that delays in positional feedback laws may serve as approximation of velocity components since $v \approx (x(t + \tau) - x(t))/\tau$. However, in our case the time delay is included only in threshold detection and so the agreement of the qualitative and quantitative nature in the case of the two types of novel Hopf-bifurcation scenarios reported in the current work is somehow surprising. A theoretical explanation for this agreement follows from the fact that for sufficiently small time delays the delayed switching line can be approximated as a position-velocity switching line provided that the time of evolution between switchings is greater than the delay time τ , which is, indeed, the case.

We should note here that similar systems have been analyzed in [1, 25] and there an onset of small scale limit cycles born around pseudo-equilibria have been also reported. However, these systems have been characterized by the presence of time delays in the position and velocity state variables as well.

Bifurcations which lead to the creation of limit cycles in switched systems, due to changes of the control strategy, have been observed in different contexts, for example due to an introduction of small hysteresis, see Sec. 2.1 in [18]. In some instances, these bifurcations can be seen as bifurcations from infinity; from the point of view of perturbations applied not to the switching, but to a state variable, see Sec. 2.2 in [18] and [10, 17] for further details. From these works, it is clear that limit cycles can be born from a pseudo-equilibrium in switched systems in a variety of scenarios and their exhaustive and unified classification seems extremely difficult. Perhaps one of the ways in which one could attempt the classification of distinct Hopf-like bifurcations in nonsmooth systems would be by considering scaling laws. That is, we should note that the bifurcation analyzed in the current manuscript differs, from example, from the Hopf-like bifurcation scenario analyzed in [9], by the scaling of the amplitude as a function of bifurcation parameter β . In the other work, the amplitude of the limit cycle born in the bifurcation grows linearly as a function of the bifurcation parameter. The question now arises whether one could

divide the Hopf-like bifurcations in switched systems into classes characterized by different scaling laws.

Future work is aimed at considering under what conditions the bifurcations analyzed in the current work are observed in higher dimensional switched systems. From the application point of view, we are interested in investigating whether there is a link between the small scale stable oscillations, born due to a small change in the character of the control law in switched models with dead-zone, and the dynamics of neuromotorcontrol systems. In particular, we are interested in understanding sway motion during quiet standing of humans affected by diabetes by linking changes of sway patterns with the bifurcations analyzed in the current work.

8 Appendix

Consider a point $\theta_0 - \theta^* = \mathcal{O}(\epsilon) < 0$. Computing

$$\frac{\partial H}{\partial t} = \frac{\partial H}{\partial \theta} \dot{\theta} + \frac{\partial H}{\partial \dot{\theta}} \ddot{\theta} = \dot{\theta} - \beta \ddot{\theta} = 0,$$

we find

$$\dot{\theta}_0 = \beta \ddot{\theta}_0 = \mathcal{O}(\epsilon),$$

since $\beta = \mathcal{O}(\epsilon)$ and $\ddot{\theta}_0 = \mathcal{O}(1)$ in a sufficiently small neighbourhood of $(\theta^*, 0)$. The subscript ‘0’ refers to a point where ψ_{IN} reaches a minimum with respect to Σ_+^ϵ . Let $H(\theta_0, \dot{\theta}_0) = H_{\min}$ and clearly $H_{\min} = \mathcal{O}(\epsilon)$. To determine the time required to reach Σ_+^ϵ from H_{\min} we may expand

$$H(\psi_{IN}([\theta, \dot{\theta}], \delta)) = H_{\min} + (H_x F_{IN})\delta + \frac{1}{2}((H_x F_{IN})_x F_{IN})\delta^2 + \mathcal{O}(\delta^3),$$

where the subscript ‘ x ’ denotes differentiation with respect to the state vector $[\theta, \dot{\theta}]$ and $H_x F_{IN}$ denotes the directional derivative of H in vector field F_{IN} . Now, $H_{\min} = \mathcal{O}(\epsilon)$ and solving $H(\psi_{IN}([\theta, \dot{\theta}], \delta)) = 0$, we find that time $\delta = \mathcal{O}(\sqrt{-H_{\min}})$ since $H_x F_{IN} = 0$ and $(H_x F_{IN})_x F_{IN} = \mathcal{O}(1)$ at $(\theta_0, \dot{\theta}_0)$.

Similar expansions may be carried out for the flow ψ_{OUT} .

References

- [1] Y. Asai, Y. Tasaka, K. Nomura, T. Nomura, M. Casadio, and P. Morasso. A model of postural control in quiet standing: robust compensation of delay-induced instability using intermittent activation of feedback control. *PLoS ONE art. no. e6169*, 4(7), 2009.
- [2] S. Banerjee and G. Verghese. *Nonlinear Phenomena in Power Electronics*. IEEE press, New York, 2001.
- [3] S. Barnett and R. G. Cameron. *Introduction to Mathematical Control Theory*. Oxford University Press, 1985.
- [4] M. di Bernardo, C. J. Budd, A. R. Champneys, and P. Kowalczyk. *Piecewise-smooth Dynamical Systems: Theory and Applications*. Springer-Verlag, 2008.
- [5] M. di Bernardo, K. H. Johansson, and F. Vasca. Self-oscillations and sliding in relay feedback systems: Symmetry and bifurcations. *International Journal of Bifurcations and Chaos*, 11(4):1121–1140, 2001.
- [6] M. di Bernardo, A. Nordmark, and G. Olivar. Discontinuity-induced bifurcations of equilibria in piecewise-smooth and impacting dynamical systems. *Physica D*, 237:119–136, 2008.
- [7] W. L. Brogan. *Modern Control Theory*. Prentice-Hall, 1991.

- [8] C. Budd, F. Dux and K. A. Cliffe. The effect of frequency and clearance variations on one-degree of freedom impact oscillators. *Journal of Sound and Vibration*, 184(3):475-502, 1995.
- [9] E. Freire, E. Ponce, F. Rodrigo, and F. Torres. Bifurcation sets of continuous piecewise linear systems with two zones. *International Journal of Bifurcations and Chaos*, 8(2):2073–2097, 1998.
- [10] P. Diamond, N. Kuznetsov and D. Rachinskii. On the Hopf bifurcation in control systems with a bounded nonlinearity asymptotically homogeneous at infinity. *Journal of Differential Equations*, 175:1-26, 2001.
- [11] P. Gawthrop, I. Loram, M. Lakie, and H. Gollee. Intermittent control: a computational theory of human control. *Biological Cybernetics*, 104:31–51, 2011.
- [12] P. Gawthrop, I. Loram, H. Gollee, and M. Lakie. Intermittent control models of human standing: similarities and differences. *Biological Cybernetics*, 108(2):159–168, 2014.
- [13] P. Kowalczyk, M. di Bernardo, A. R. Champneys, S. J. Hogan, M. Homer, Yu. A. Kuznetsov, A. B. Nordmark, and P. T. Piironen. Two-parameter nonsmooth bifurcations of limit cycles: classification and open problems. *International Journal of Bifurcation and Chaos*, 16(3), 2006.
- [14] P. Kowalczyk, P. Glendinning, Martin Brown, Gustavo Medrano-Cerda, Houman Dallali, and Jonathan Shapiro. Modelling human balance using switched systems with linear feedback control. *Journal of the Royal Society Interface*, 9:234–245, 2011.
- [15] Yu. A. Kuznetsov, S. Rinaldi, and A. Gragnani. One-parameter bifurcations in planar filippov systems. *Int. J. Bifurcation Chaos*, 13:2157–2188, 2003.
- [16] R.I. Leine. *Bifurcations in Discontinuous Mechanical Systems of Filippov-Type*. PhD thesis, Technische Universiteit Eindhoven, The Netherlands, 2000.
- [17] J. Llibre, and E. Ponce. Bifurcation of a periodic orbit from infinity in planar piecewise linear vector fields. *Nonlinear Analysis*, 36:623-653, 1999.
- [18] O. Makarenkov and J. Lamb. Dynamics and bifurcations of nonsmooth systems: A survey. *Physica D: Nonlinear Phenomena*, 241(22), pp.1826-1844, 2012.
- [19] J. Milton, T. Insperger, and G. Stépán. Chapter: Human Balance Control: Dead Zones, Intermittency, and Micro-Chaos. Pages 1 to 28 in: *Mathematical Approaches to Biological Systems*, Springer 2015.
- [20] J. Milton, T. Ohira, J. Cabrera, R. Fraiser, J. Györfy, F. Ruiz, M. Strauss, E. Balchand P. Marin, and J. Alexander. Balancing with vibration: A prelude for “drift and act” balance control. *PLoS ONE*, 4(e7427), 2009.
- [21] A. B. Nordmark and P. Kowalczyk. A codimension-two scenario of sliding solutions in grazing-sliding bifurcations. *Nonlinearity*, 19(1) pp. 1-26, 2006.
- [22] K. Popp, N. Hinrichs, and M. Öestreich. Dynamical behaviour of friction oscillators with simultaneous self and external excitation. *Sadhana (Indian Academy of Sciences)*, 20:627–654, 1995.
- [23] J. Sieber. Dynamics of delayed relay systems. *Nonlinearity*, 19:2489–2527, 2006.
- [24] J. Sieber, P. Kowalczyk, S. J. Hogan, and M. di Bernardo. Dynamics of symmetric dynamical systems with delayed switching. *Journal of Vibration and Control*, 16:1111–1140, 2010.
- [25] D. J. W. Simpson, R. Kuske, and Y.-X. Li. Dynamics of simple balancing models with time-delayed switching feedback control. *Journal of Nonlinear Science*, 22(2):135–167, 2012.

- [26] M. Tanelli, G. Osorio, M. di Bernardo, S. M. Savaresi and A. Astolfi Existence, stability and robustness analysis of limit cycles in hybrid anti-lock braking systems. *International Journal of Control*, 82(4):659–678, 2009.